Master's Thesis MEE10:85

Implementation and Evaluation of NIST Biometric Image Software for Fingerprint Recognition

Sainath Maddala

Sreekanth Rao Tangellapally

Examination

Master of Science in Electrical Engineering Technology

Blekinge Institute of Technology

September 2010

School of Engineering
Department of Electrical Engineering
Blekinge Institute of Technology, Sweden
Supervisor : Josef Ström Bartunek
Examiner : Mikael Nilsson

Implementation and Evaluation of NIST Biometric Image Software for Fingerprint Recognition

This thesis is presented as part of Double Degree Master of Technology and Master of Science in Electrical Engineering with emphasis on Signal Processing.

Contact Information:
Authors:
Sainath Maddala
email: sainath.32@gmail.com
Sreekanth Rao Tangellapally
email: sris.chinnu@gmail.com

Supervisor:
Josef Ström Bartunek
School of Engineering (ING)
Dept of Electrical Engineering,
Blekinge Institute of Technology, Sweden
email: josef.strombartunek@bth.se

Examiner:
Mikael Nilsson
School of Engineering (ING)
Dept of Electrical Engineering,
Blekinge Institute of Technology, Sweden
email: mikael.nilsson@bth.se

Abstract

Fingerprints are rich in details which are in the form of discontinuities in ridges known as minutiae and are unique for each person. The main desire of this thesis is to implement and evaluate National Institute of Science and Technology (NIST) Biometric Image Software (NBIS) for fingerprint recognition using C language MEX-files. NBSI source code is written in ANSI C programming language. A system developed in Matlab environment using C language MEX-files is used for implemented and evaluated the NIST source code. Minutiae extraction and minutiae matching are performed by using a function developed with NBIS. The extracted minutiae are passed through the function with NBIS that match two minutiae patterns and produce a match score. Finally the performance of the system is evaluated on various fingerprint databases and results are presented in Receiver Operating characteristics (ROC) graphs.

ACKNOWLEDGMENT

First of all we would like to thank our supervisor JOSEF STRÖM BARTUNEK for giving the opportunity to work on this topic and guiding us until the final stage of the thesis work. The meetings with him during the most difficult times have been fruitful in finding solutions to our queries and problems we encountered time to time.

We are thankful to MIKAEL NILSSON for allotting time in busy schedule and giving lectures on ROC graphs. These lectures helped us in the practical part of our work.

Last but not least, we are thankful to our beloved parents and friends in India for inspiring us all through our stay in Sweden and supporting us. Without them nothing would not have been possible. Thank you very much!

Sainath Maddala,
Sreekanth Tangellapally,
2010, Sweden.

Contents

List Of Figures

Chapter 1

Introduction

1.1 Biometrics

"Biometrics" (bios metron = "life measurement") is defined as the automated methods of identifying or authenticating the identity of a living person based upon one or more intrinsic physical or behavioral traits. A number of biometric technologies have been developed and are being used in numerous applications such as secure identification and personal verification solutions etc. Some examples of different biometrics are fingerprints, face recognition, iris, retina scan, signature etc. "Although biometrics emerged from its extensive use in law enforcement to identify criminals (e.g., illegal aliens, security clearance for employees for sensitive jobs, fatherhood determination, forensics, and positive identification of convicts and prisoners), it is being increasingly used today to establish person recognition in a large number of civilian applications" [19].

1.2 Fingerprints History

Human fingertips are fully formed at about seven months of fetus development and ridge configurations which form distinctive patterns. Patterns on fully developed fingerprints do not change throughout the life of an individual except due to accidents such as bruises and cuts on the fingertips. Print of these patterns is known as fingerprints [1]. Fingerprinting first created by a British surgeon called Dr. Henry Fault. In late nineteenth century Sir Francis Galton discovered some of the points or characteristics from which fingerprints can be identified. Hence the term "Fingerprint identification" is founded by the Galton points for the science technology. Fingerprint identification began its transition to automation in the late 1960. In 1969, the Federal Bureau of Investigation (FBI) developed a system to automate fingerprint identification. This is first used for manual process and then it is connected to National Bureau of Standards (NBS) known as National Institute of Standards and Technology (NIST). NIST is an organization to study the process of automating fingerprint classification, feature extraction and matching. It identifies two key challenges:

1. Scanning fingerprint cards and extracting minutiae from each fingerprint.
2. Feature extraction, comparing and matching list of minutiae against list of large repositories of fingerprints [2].

In the early 1990's, NIST began developing a system to enable the electronic exchange of fingerprint records and images by law enforcement agencies. Also to handle electronic transactions with these agencies which is called the Integrated Automated Fingerprint Identification System (IAFIS) [3]. In 1994 three major challenges are identified and investigated:

1. Digital fingerprint acquisition.
2. Local ridge characteristic extraction.
3. Ridge characteristic pattern matching.

At present fingerprint verification systems began to appear of various access control and verification functions.

One of the most important tasks considering an automatic fingerprint recognition system is the minutiae biometric pattern extraction from the captured image of the fingerprint [4]. The capture device returns an image, usually with 256 grey-levels, which consists of dark (ridges) and bright (valleys) lines. The most widespread fingerprint matching approach relies on the uniqueness of a fingerprint's prominent singular points known as minutiae. These minutiae are represented either by bifurcation or termination of ridges. A fingerprint image is captured in one of two ways shown in Fig. 1.1.

1. Scanning an inked impression of a person's finger
2. Using a live-scan fingerprint scanner.

(a) **(b)**

Figure 1.1: (a) Inked impression fingerprint (b) Live-scanned fingerprint.

1.3 Fingerprint Classification

Over the past few decades, a large scale of fingerprint recognition techniques has been proposed by researches for distinguishing fingerprint classes. Classifying a fingerprint

images is a very difficult pattern recognition problem, due to the small interclass variability, the large intraclass variability, the presence of noise and the ambiguous properties of fingerprints. Adopting a classification approach can greatly reduce the number of comparisons during fingerprint retrieval and consequently reduce the response time of the identification process. As an increasing database of fingerprint images, it became important to have an efficient method of classifying the fingerprints. The most widely used classification method is based on Henry's classification which consists of eight classed: Plain Arch, Tented Arch, Left Loop, Right Loop, Plain Whorl, Central-Pocket Whorl, Double Loop Whorl and Accidental Whorl. Fig. 1.2 shows basic categories of fingerprint classes [5].

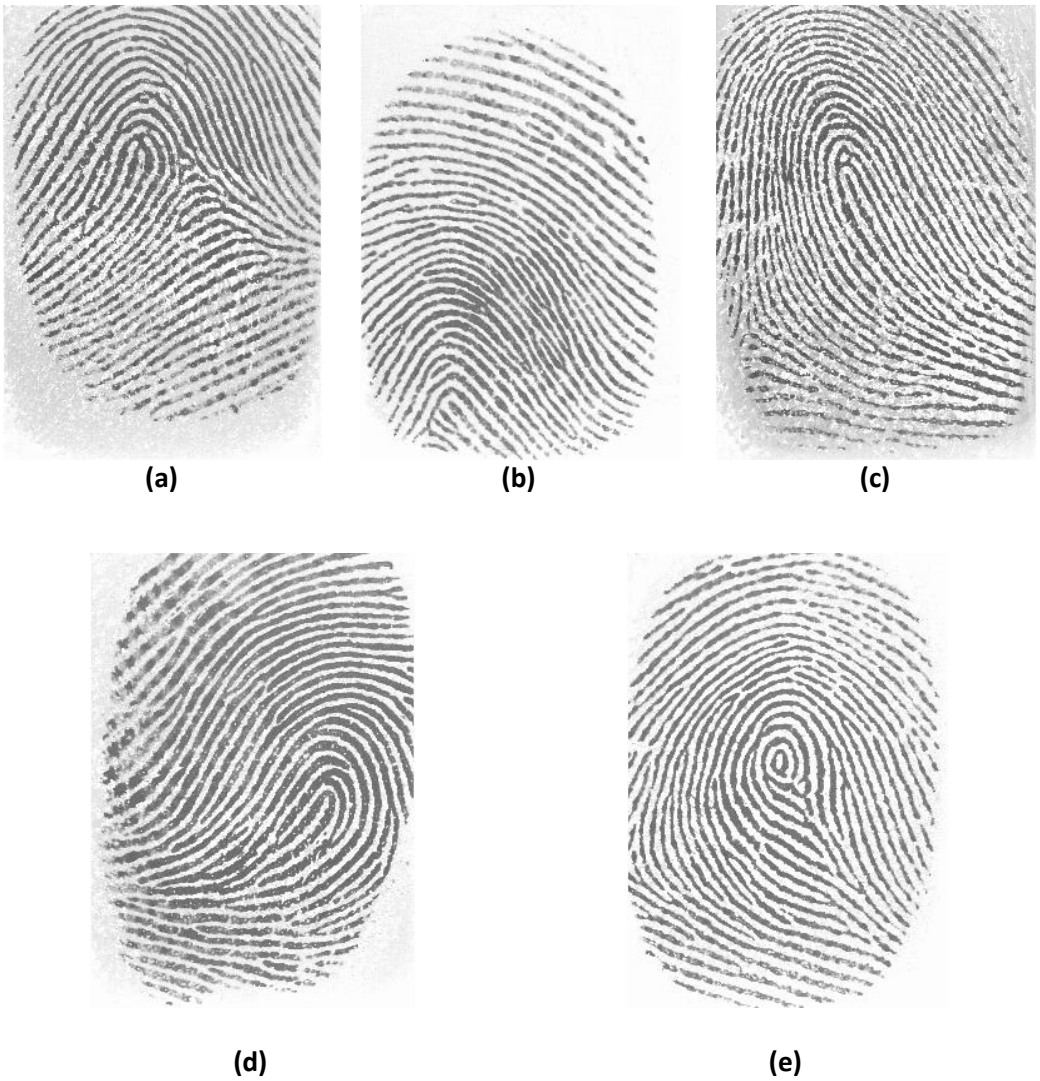

Figure 1.2: Tented Arch (b) Arch (c) Right Loop (d) Left Loop (e) Whorl.

Another major challenge is related to the presence of noise in fingerprint images. Noise fingerprint will make the classification task more difficult even for a human expert. Random noise and other effects caused by the skin conditions such as dry, sweaty, dirty, and diseased will degrade quality of fingerprint images. Recovering original ridge patterns from the fingerprint is important. This can be done by performing pre-processing operation on fingerprint. Hence proposed fingerprint classification algorithm rejects such images because this would be less damaging than a wrong decision. For this reason, several classification approaches include a rejection mechanism, which improves the accuracy at the cost of discarding some fingerprints.

1.3.1 Fingerprint Analysis

The fingerprints, when analyzed at different scales, produce different types of features. At global level, patterns known as ridges and valleys exhibits a number of particular shapes called singularities, which are classified as: loop, delta and whorl. At the local level, ridge characteristics, called minutia. There are several types of minutiae, but the two most prominent ridge characteristics are: ridge ending (point where ridge ends abruptly) and ridge bifurcation (points where ridge forks or diverges into branch ridges) as shown in Fig. 1.3. The rest of the minutiae are combination of each or those two types. A good quality of image may have between 40 to 100 of minutia, each described by its location (x, y coordinates) and its orientation (θ).
.

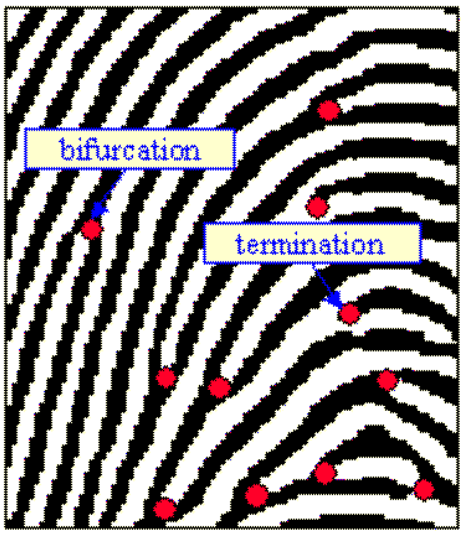

Figure 1.3: Fingerprint image with bifurcations and terminations marked out.

1.3.2 Fingerprint Recognition

Fingerprint classification and matching are key parts in an automated fingerprint recognition system. The fingerprint matcher compares features from the input search point against all appropriate records in the database to determine if a probable match exists. There are various approaches of automatic fingerprint matching that have been proposed which include minutiae based approaches, and image based approaches. Minutia based approaches are the most popular ones being included in almost all contemporary fingerprint identification and verification system.

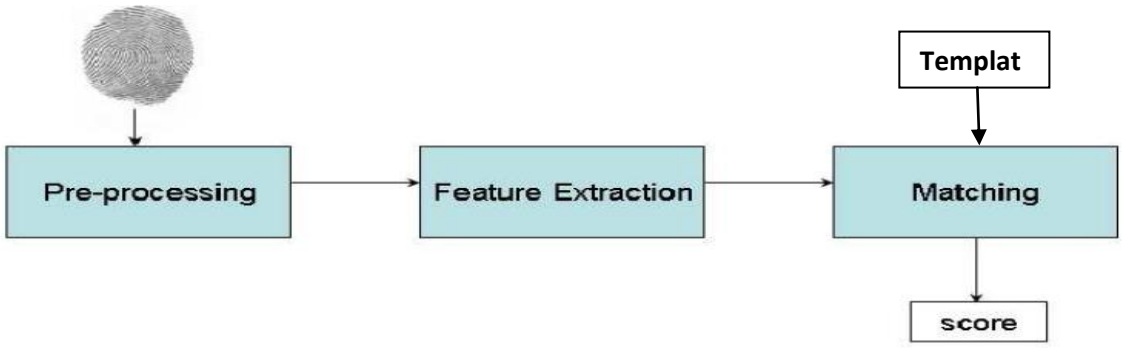

Figure 1.4: Main modules of Fingerprint verification system.

Fingerprint verification problem is divided into two main tasks:
1. Minutiae extraction.
2. Minutiae matching.

The various modules of fingerprint verification system are shown in Fig. 1.4 .The first stage consists of fingerprint sensing which has been historically carried out by spreading the finger with ink and pressing it against a paper card and then scanned, resulting in a digital representation. This process is known as off-line acquisition and is still used in law enforcement applications. Currently, it is possible to acquire fingerprint images by pressing the finger against the flat surface of an electronic fingerprint sensor. This process is known as online acquisition. Acquired image may contain noise that is removed in pre-processing stage and minutiae are extracted from pre-processed image. Final stage for fingerprint matching is performed by passing minutiae patterns of the fingerprint to matcher. This matcher will produce a match score based on fingerprint matching.

1.4 Fingerprint Database

Research in biometrics profoundly depends on the availability of sensed data. The growth that the field has experienced over the past two decades has led to the appearance of increasing numbers of biometric databases. Previous to the International Fingerprint Verification Competitions (FVC) [20], the only large, publicly available datasets were the NIST databases [6]. However, these databases were not well suited for the evaluation of algorithms operating with live scan images [1]. The evaluation of the implemented NBIS system is performed on available biometric databases that include the fingerprint trait acquired with live-scan sensors.

1.5 Outline

The main aim of this thesis is to implement and evaluate of NIST Biometric Image Software for fingerprint recognition in MATLAB environment. The NBIS source code is entirely written in ANSI C programming language. NBIS is implemented in C language MEX-files to run in MATLAB. First fingerprint image is enhanced and minutiae are extracted. The extracted minutiae are passed through the function that match two minutiae patterns and produce a match score. Performance of the system is evaluated on various fingerprint databases and the results obtained are presented in Receiver Operating Characteristics (ROC) graphs.

Chapter 2

Minutiae Extraction

2.1 Introduction

Minutiae extraction of the fingerprint is performed by using the algorithm developed by NIST. Flowchart in Fig. 2.1 explains the minutiae extraction process from the fingerprint. In the first stage Image maps are generated from the input fingerprint. The quality maps indicate internal quality of the fingerprint. The values 0-4 mark different conditions (low contrast, high contrast, high curvature, low ridge flow) within the fingerprint [15]. These values help in removing the false minutiae from the fingerprint. In the second stage image binarization is performed and the minutiae are detected from the binarized fingerprint image. Removal of false minutiae from the fingerprint are based on the quality factor. After removing false minutiae the minutiae which are left are known as real minutiae.

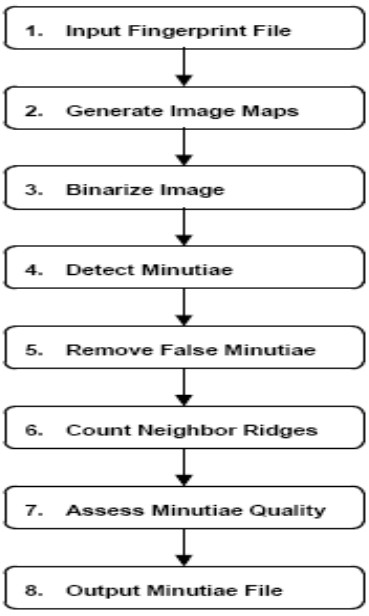

Figure 2.1: Minutiae detection process [15].

2.2 Operations Performed on Fingerprint

Minutiae from the fingerprint image can be extracted directly from the fingerprint. However the extraction process is difficult and not accurate due to noise present in the fingerprint image. Also the intensity of the line pattern may differ between fingerprints. Due to these reasons the extracted minutiae from the fingerprint may contain both real and false minutiae. To minimize extraction of false minutiae from the fingerprint image a pre-processing and post-processing stage is performed to complement the minutiae extraction. Fig. 2.2 shows operations performed for extracting real minutiae from fingerprint.

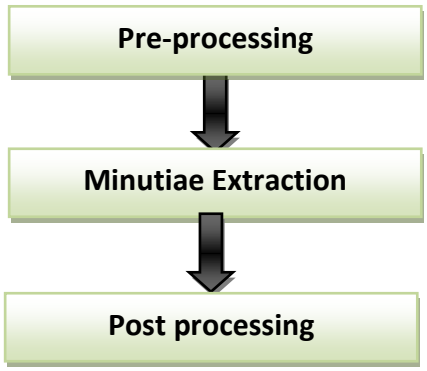

Figure 2.2: Flowchart representing operations performed before and after extracting minutiae.

2.3 Pre-Processing

Pre-processing operation is used for enhancing the contrast of the fingerprint image. Quality of the acquired fingerprint depends on the condition of the finger and sensor used. Both factors may lead to poor quality between ridges, crossovers and bifurcation in the fingerprint image. So pre-processing operation should be performed before extracting the minutiae from the fingerprint. Pre-processing operation can be performed with various methods. For example histogram equalization will increase the contest of the image. The function trim_histtails_contrast_boost() developed by NIST use histogram modulation for increasing the contrast of the fingerprint image. Quality of the image can also be increased by using the filters. Low pass filter decrease the noise from the image, band pass filter decrease undesired noise from orientations which helps in preserving true ridges [14]. Image enhancement can also be performed using Fourier transform based method [15].

2.3.1 Fingerprint Enhancement using Fourier Transform

Divide the fingerprint image into sequence of squares each of size *32X32* pixels and perform a 2 dimensional fast Fourier transform ($2D\ FFT$) to the fingerprint image. Next the nonlinear function is applied to increase the power of useful information (orientation of ridges and valleys, to decrease noise etc). Where the nonlinear function is performed by multiplying the FFT of the block by its magnitude a set of times to increase the strength of the frequencies. Then inverse $2D$ FFT is applied to transform the enhanced data to spatial representation. Fig. 2.3 shows the enhanced image using Fourier transform method [15].

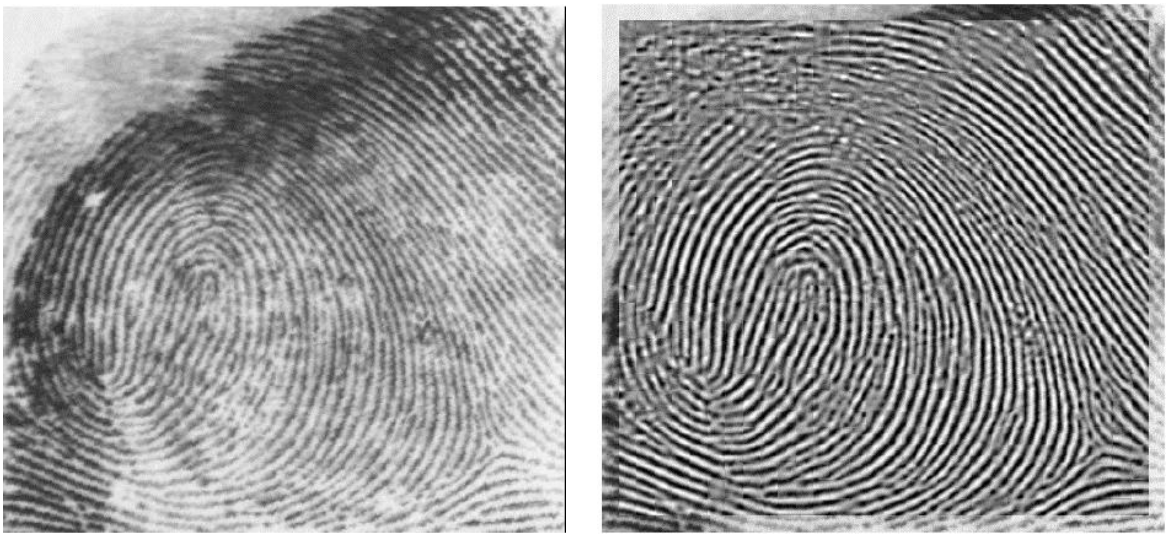

(a) (b)

Figure 2.3: (a) Fingerprint after segmentation, (b) Fingerprint enhanced using Fourier transform method.

2.3.2 Fingerprint Enhancement using Histogram Equalization

In this work trim_histtails_contrast_boost() function developed by NIST is used for fingerprint enhancement. This function computes and analizes the pixel intensity histogram and expands pixel intensities across computed intensity range. First lower pixel limit and upper pixel limit values are computed then each pixel intensity in the fingerprint is observed. If the pixel intensity is lower than lower pixel limit then reset pixel intensity to lower limit and in the same way if the pixel intensity is grater than upper pixel limit then reset pixel intensity to upper limit. Fig. 2.4 shows original image and enhanced image using _histtails_contrast_boost() function.

(a) (b)

Figure 2.4: Fingerprint obtained after preprocessing (a) Original image (b) Enhanced image.

2.4 Minutiae Extraction

2.4.1 Definition of Minutiae

Basic fingerprint image consists of ridges, valleys, cores, deltas, pores etc as shown in Fig. 2.5a. The ridge endings and ridge bifurication's are used for comparing two fingerprints with each other, denoted minutiae based matching. Commonly pixel with one neighbor is treated as ridge ending and the pixel with three neighbors is treated as ridge bifurcation. Fig. 2.5b illustrates ridge ending and ridge bifurcation which plays a vital role in fingerprint detection known as real minutiae. These ridge ending and ridge bifurcation do not change over time, therefore well suited for fingerprint matching. Fingerprint usually consists of *40* to *100* minutiae points. Minutiae location is represented by a coordinate location of the fingerprint image. Different systems represents minutiae location differently. ANSI/NIST standard for locating minutiae is explained in section 2.3.2.

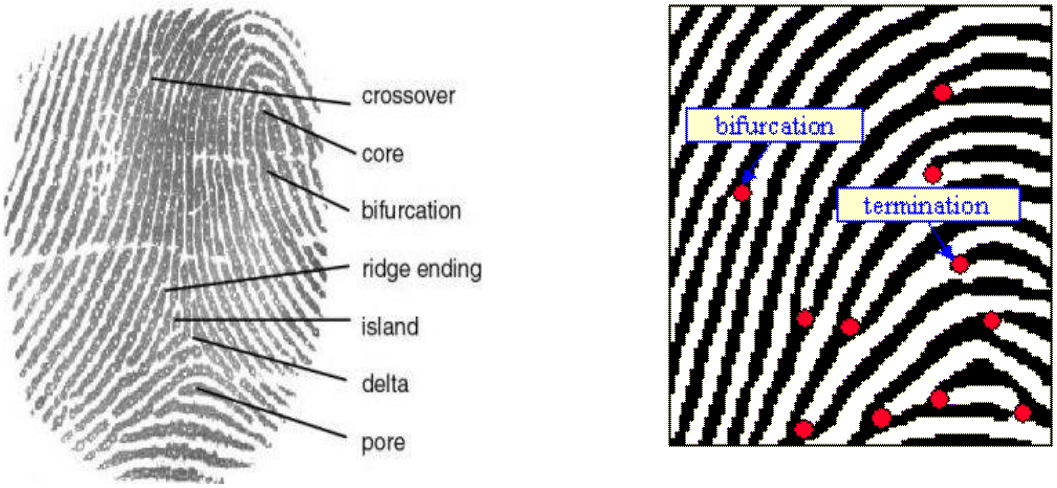

Figure 2.5: a) Basic fingerprint image, b) Fingerprint image with bifurcations and terminations.

2.4.2 Detecting Minutiae Position and Orientation

Detection of minutiae from the fingerprint requires conversion of grayscale image into binarized image where black pixels represents ridges and white pixels represents valleys. This grayscale image conversion process is known as binarization. For this process each pixel in the image must be analyzed for assigning white and black pixel. First the binary image is scanned to identify ridge endings and ridge bifurcation. Patterns scanning are performed both horizontally and vertically. The *2x3* pixel pattern is used for scanning the image. Patterns represented in Fig. 2.6 illustrate procedure for detecting the minutiae points in the binarized fingerprint image. Two patterns in the

Fig.2.6 represents ridge endings and rest represents bifurcations.

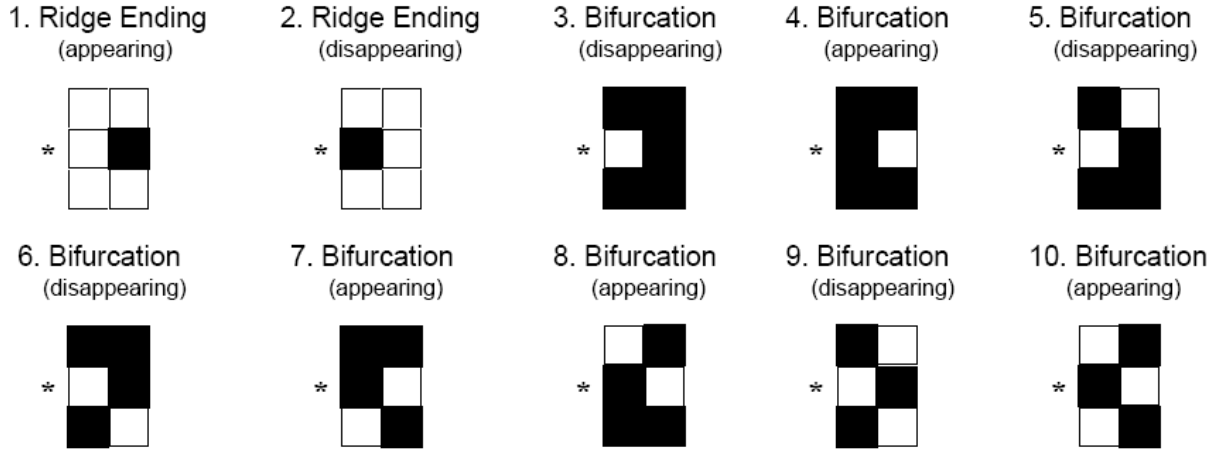

Figure 2.6: Pixel patterns used to detect minutiae.

The coordinates and orientation of each ridge endings and bifurcations are essential for fingerprint matching. ANSI/NIST specifies units in degrees of $0.01mm$ from origin in the bottom left corner of the image. For example, if an image of size *500X600* is scanned at *19.69* pixels per millimeter (ppmm) with units $0.01mm$ is

$$(2539,3047) \quad = \quad \left(\frac{500}{19.69*0.01} X \quad \frac{600}{19.69*0.01} \right). \tag{2.1}$$

Pixel coordinates (100,150) represented in standard units as

$$(507, 2284) \quad = \quad \left(\frac{100}{19.69*0.01}, \quad 3047 - 1 - \frac{150}{19.69*0.01} \right). \tag{2.2}$$

Minutiae orientation is represented in degrees. Horizontal axis from ridge ending and ridge bifurcation represents zero degrees and increasing angle in counter-clockwise. Orientation of ridge ending is the angle between line projected at the ridge ending and horizontal axis [15]. Orientation of bifurcation is the angle between line projected at the middle of ridge bifurcation and horizontal axis is as shown in Fig. 2.7.

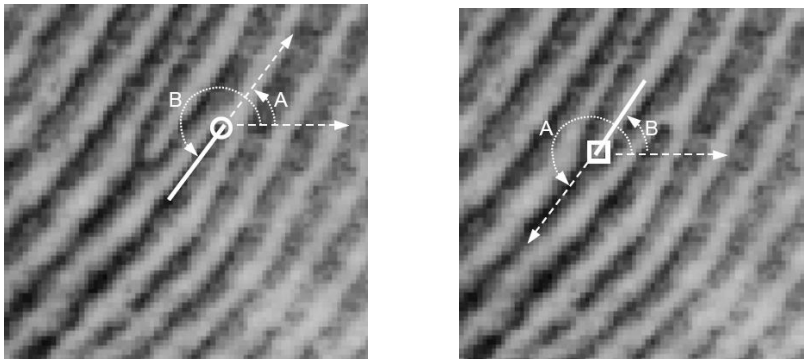

Figure 2.7: Minutiae Orientation.

Minutiae detected in the fingerprint are as shown in the Fig. 2.8 which may consist of real and false minutiae. The number of falsely detected minutiae can be minimized in post-processing stage with the help of quality factor. The function get minutiae() contains the algorithm for minutiae detection/extraction which is developed by NIST . Operations explained in section 2.4.2 are performed internally.

Figure 2.8: Real and false minutiae detected in the fingerprint.

2.5 Post processing

Minutiae extracted from the fingerprint consist of real and false minutiae as shown in Fig. 2.8. The number of falsely detected minutiae depends upon the quality of the fingerprint. These false minutiae much be filtered to remove as many false minutiae as possible without removing real minutiae. The redundant minutiae in the fingerprint are of the form

a) Minutiae Points adjacent to each other

b) Minutiae near the borders

c) Spike, break, bridge, hole as shown in the Fig. 2.9.

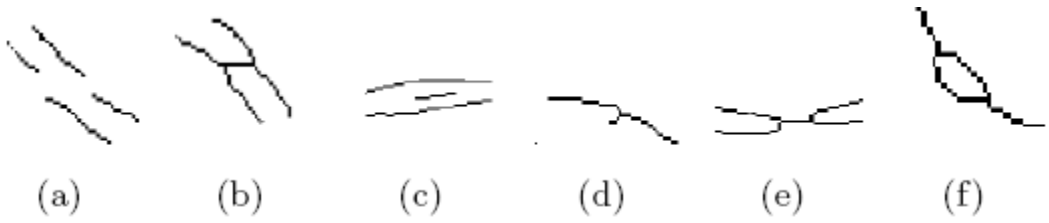

Figure 2.9: (a) Broken ridges, (b) Bridge, (c) Short ridge, (d) Short ridge, (e) Short Ridge, (f) Hole.

These types of false minutiae may cause serious problem during matching. Removing all false minutiae separately is time taking and complex. For this reason quality of each minutiae is computed. First reliability measure is calculated based on pixel intensity statistics (man and standard deviation) within the immediate neighborhood of the minutiae point. The size of neighborhood is set to 11 pixels. For high quality region will cover full grayscale spectrum. Reliability R, is calculated by using the parameters $F\mu, F\sigma$, where $F\mu, F\sigma$ are calculated by using neighborhood mean, μ, and standard deviation, σ [15]. Pixel intensities of ideal neighborhood of the fingerprint will have standard deviation ≥ 64.

$$F\mu = 1.0 - \frac{|\mu - 127|}{127} \tag{2.3}$$

$$F\sigma = \begin{cases} 1.0 \; if \; \sigma > 64 \\ \frac{\sigma}{64} \quad otherwise \end{cases} \tag{2.4}$$

$$R = \min(F\mu, F\sigma). \tag{2.5}$$

Minutiae quality Q is calculated using reliability R as:

$$Q = \begin{cases} .50 + (.49 * R) & if \; L = 4 \\ .25 + (.24 * R) & if \; L = 3 \\ .10 + (.14 * R) & if \; L = 2 \\ .05 + (.04 * R) & if \; L = 1 \\ .01 & if \; L = 0 \end{cases} \tag{2.6}$$

and the quality value ranges between *0.01* to *.99* [15]. L is the location of the minutiae point within the quality map. Minutiae with lower quality correspond to false minutiae and minutiae with high quality correspond to real minutiae. The false minutiae in the fingerprint can be removed by keeping proper threshold value. The minutiae which are less than the threshold are not allowed i.e. lower quality(false minutiae) and rest of the minutiae which fulfils the threshold value are allowed i.e. high quality(real minutiae). Minutiae obtained are plotted on the fingerprint Fig. 2.10.

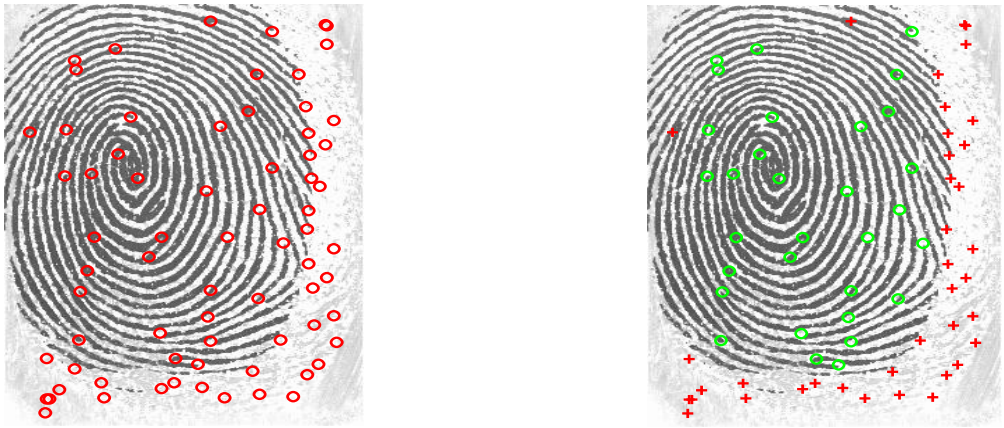

(a) (b)

Figure 2.10: a) Fingerprint image containing both false and real minutiae, b) Fingerprint image containing real minutiae with "*o*" in green and false minutiae with " + "in red.

Chapter 3

Fingerprint Matching

3.1 Introduction

Fingerprint matching is the process of matching two fingerprint images. Matching may be from same person or from different person. If the matching is from same person it is known as genuine match and if the matching is from different persons it is known as imposter matching.

3.2 Factors responsible for intra-class variations

Reliably matching fingerprint images is an extremely difficult problem, mainly due to large variability in different impressions of the same finger. Displacement, rotation, non-linear distortion, noise and feature extraction errors are the main factors responsible for intra-class variations. Due to this reasons fingerprints from the same finger may sometimes appear quite different whereas fingerprints from different fingers may appear quite similar (see Figure3.1)

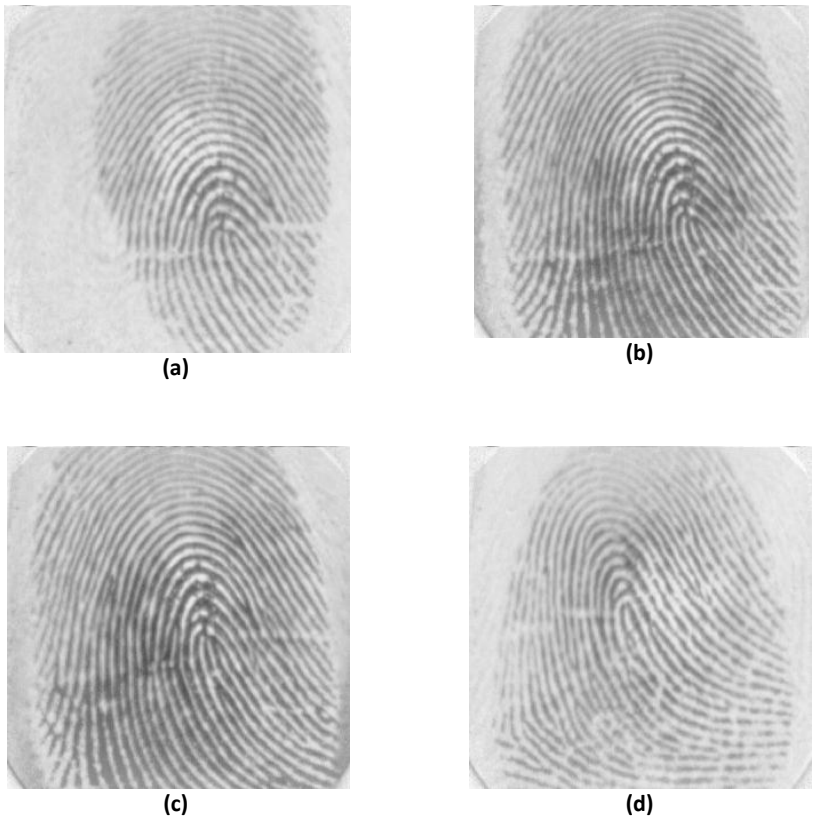

Figure 3.1: Fingerprint images in a) and b) appear different, however, the impressions are of same finger c) & d) appear similar; however, they are from different fingers.

3.3 Fingerprint matching

Fingerprint matching is a difficult approach due to quality variations of the fingerprint from the same user in time. These variations are due to changing skin conditions, noise, errors caused during extraction. Some of the fingerprint matching techniques are

- Correlation-based matching,
- Minutiae-based matching,
- Ridge feature-based matching.

3.3.1 Correlation-based matching

Two fingerprint images are superimposed and the correlation (at the intensity level) between corresponding pixels is computed for different alignments. This method is gaining good results in matching fingerprint patterns in authentication process. High matching accuracy can be obtained with this method. In correlation method gray-level information is taken and the matching of the fingerprint's are performed [13].

Correlation based approach is the alternative approach when the fingerprint image is not good, in this situation's extracting minutiae may cause problem. However, correlation based approach cannot be used in various applications due to its large computational effort.

3.3.2 Minutiae-based matching

In minutiae based matching depends on position and orientation of minutiae points obtained from fingerprint. How to find the minutiae coordinates and orientation has been explained in chapter 2. In this work, minutiae based fingerprint detection is performed by using the BOZORTH3 algorithm developed by NIST. This algorithm generates a score based on pairing minutiae of the fingerprints. Total operation of BOZORTH3 is explained in section 3.4.

3.3.3 Ridge feature-based matching

Ridge feature maps could also be used for fingerprint matching [18]. Utilizes both orientation and frequency information, eliminates the need of minutiae detection in fingerprint.

Minutiae extraction is difficult in low-quality fingerprint images, whereas other features of the fingerprint ridges pattern (local orientation and frequency, ridge shape) may be extracted more reliably than minutiae. The approaches belonging to this category compare fingerprints in terms of feature extraction from the ridge pattern.

3.4 BOZORTH3

BOZORTH3 is an algorithm and utility that matches two minutiae patterns with each other and produces a match score. Matching between the fingerprint can be one-to-one verification or one-to-many identification. Bozorth algorithm includes three steps for fingerprint matching:

Step 1: Construction of Intra-Fingerprint Minutiae Comparison Tables

Step 2: Construction of Inter-Fingerprint Compatibility Table

Step 3: Traverse Inter-Fingerprint Compatibility Table constructed in second step

In step 1 probe fingerprint comparison table and gallery fingerprint comparison table are constructed. Table construction for both galley and probe fingerprint mainly depends on position and orientation of minutiae. Relative measurements from each minutiae to all other minutiae are computed in a fingerprint and tabulated in the table known as minutiae comparison table. Relative measurements of minutiae in a fingerprint to find the distance between the minutiae and orientation of the fingerprint.

Consider Fig.3.2 in which k and j represents minutiae points on fingerprint. Consider point k where k (x_k, y_k) represents location of minutiae k on the fingerprint and $\beta 1$ represents the orientation θ_k of minutiae. All the minutiae of the fingerprint are represented in this style. In Fig. 3.2 $d(pm)$ represents the distance between two minutiae's k, j as distance between two minutiae's will remain constant regardless of how much shifting and rotation may exist between two points. β_k, β_j are computed relative to the intervening line as shown by incorporating θ_kj and each minutiae's orientation t[16].

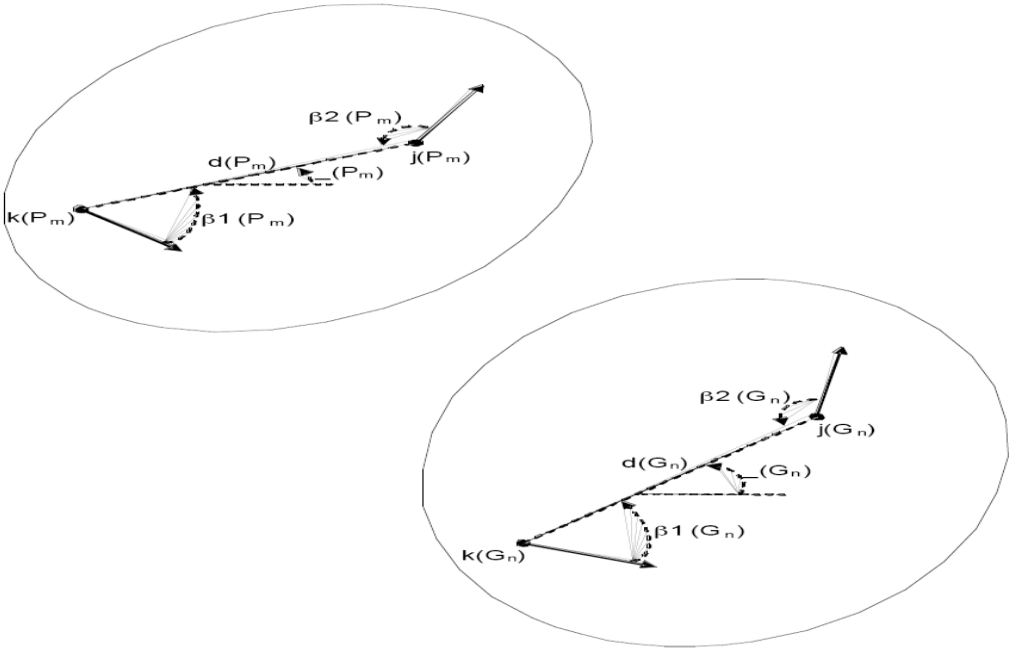

Figure 3.2: Intra-Fingerprint minutiae comparison.

For each comparison between minutiae all the entries mentioned below are made

$\{d\_kj, \beta\_k, \beta\_j, \theta\_kj\ \}$ Where $\beta\ 1 = min(\beta\_k, \beta\_j)$ and$\beta\ 2 = max(\beta_k, \beta_j)$ in the illustration above $\beta 1\ =\ \beta\_k\ and\ \beta 2\ =\ \beta\_j$. Entries made in the table are stored in order of increasing distance and the table is trimmed at the point when the maximum distance threshold is reached. Same procedure is followed for each fingerprint while constructing Intra-Fingerprint Minutiae Comparison Table [16].

In step 2 compatible table is constructed from two separate fingerprint comparison tables. All vales of probe fingerprint comparison table are pair-wise computed with measurements stored in comparison table P. All the measurements are stored as mth entry in table P, denoted as pm and $k(pm)$ represents the measurements corresponding to minutiae k. Distence between two minutiae is also store in table as $d(P_m)$. The same procedure is done for gallery fingerprint and is stored in table entry Gn. Following tests are performed on table entries Pm and Gn to form a compatible table.

$$\Delta\mathrm{d}\big(\mathrm{d}(\mathrm{pm}),\mathrm{d}(\mathrm{Gn})\big) < T\mathrm{d} \tag{3.1}$$

$$\Delta\beta\big(\beta1(\mathrm{pm}),\beta1(\mathrm{Gn})\big) < T\beta \tag{3.2}$$

$$\Delta\beta(\beta2(\mathrm{pm}),\beta2(\mathrm{Gn})) < T\beta. \tag{3.3}$$

These tests checks if the corresponding distances and angles are in specified tolerance. Where $\Delta\beta()$ and $\Delta d()$ represents the difference function.

Step 3 determines how well two fingerprints match each other based on the compatibility table designed in step 2.

3.5 Results obtained for Genuine and Imposter matching

First minutiae tables are constructed for both probe and gallery fingerprint as shown in Fig.3.3. In the table X, Y represents the coordinates of each minutiae, T represents orientation θ and D represents the minutiae quality. These tables containing all minutiae parameters are then passed to the minutiae matcher for generating the scores. *S(P1,P2)* represents scores obtained from genuine matach where $P1$ and $P2$ are the fingerprints from same person. $S(G1, G2)$ represents scores obtained from imposter matach where $G1$ and $G2$ are the fingerprints from different persons. As larger the matching score, the fingerprints are more likely from the same person.

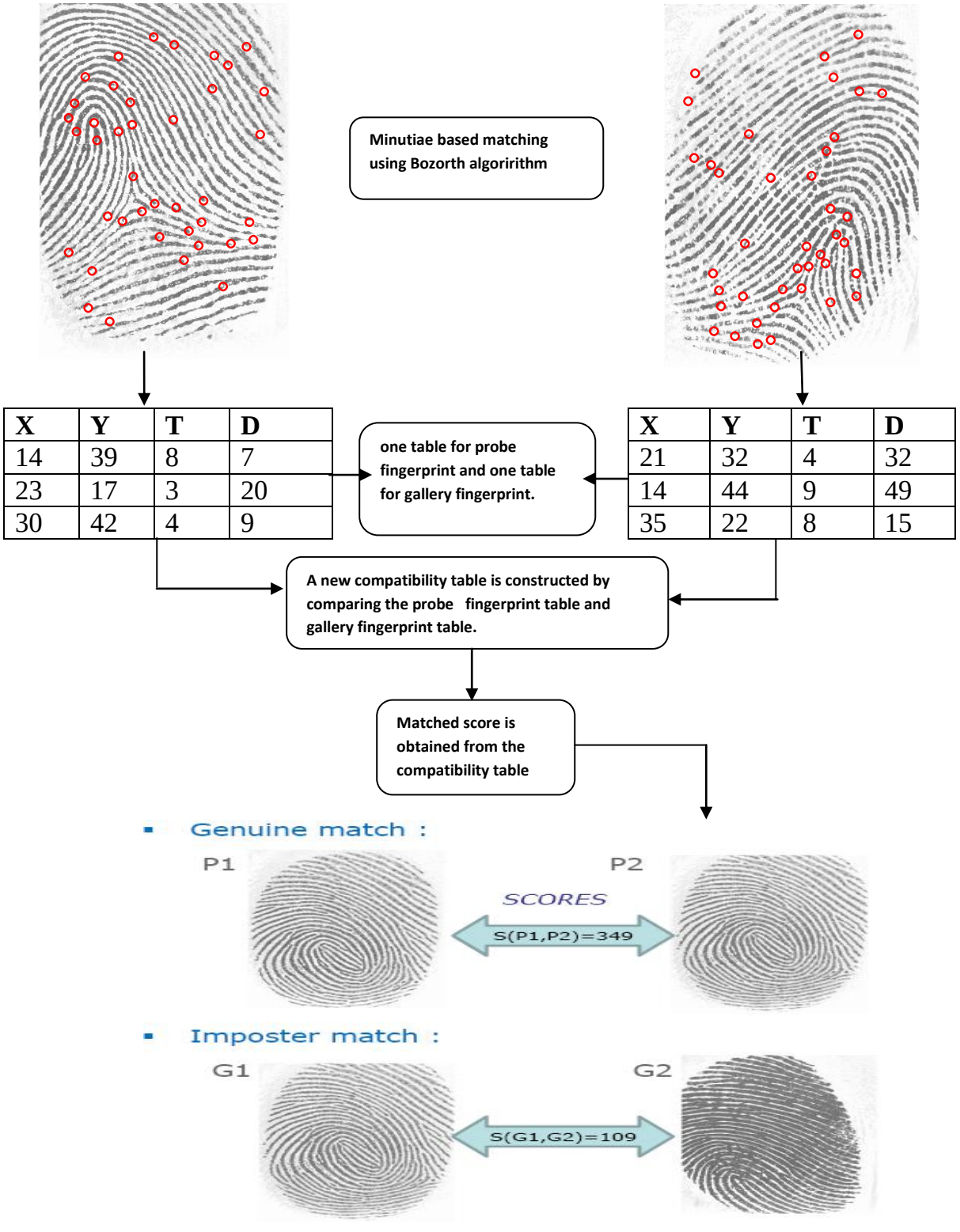

Figure 3.3: Flowchart illustrating minutiae matching process.

Chapter 4

MEX-Files

4.1 Introduction

Algorithms written in c programming language are possible to reuse in MATLAB through MEX-Files. Algorithms developed by NIST for minutiae extraction and fingerprint matching are written in C programming language, however, converting the source files written in C language into Matlab script is very complex and waste of time. To overcome this problem MEX-Files are used.

4.2 Components of a C MEX-file

The source code for a MEX-file consists of two distinct parts.

- Computational routine.
- Gateway routine.

Computational routine helps in performing the computations that are implemented in the MEX-file and it may be numerical computations, inputting and outputting data.

Gateway routine helps in interfacing the computational routine with Matlab using mexFunction and its parameters prhs, nrhs, plhs, nlhs where

Prhs is an array of right-hand input arguments,

Nrhs is number of right-hand input arguments,

Plhs is an array of left-hand output arguments and

Nlhs is number of left-hand output arguments.

In gateway routine, data can be access by using mxArray structure and data manipulation is in C computational subroutine. Flowchart shown in Fig. 4.1 shows the working procedure of MEX-Files in Matlab.

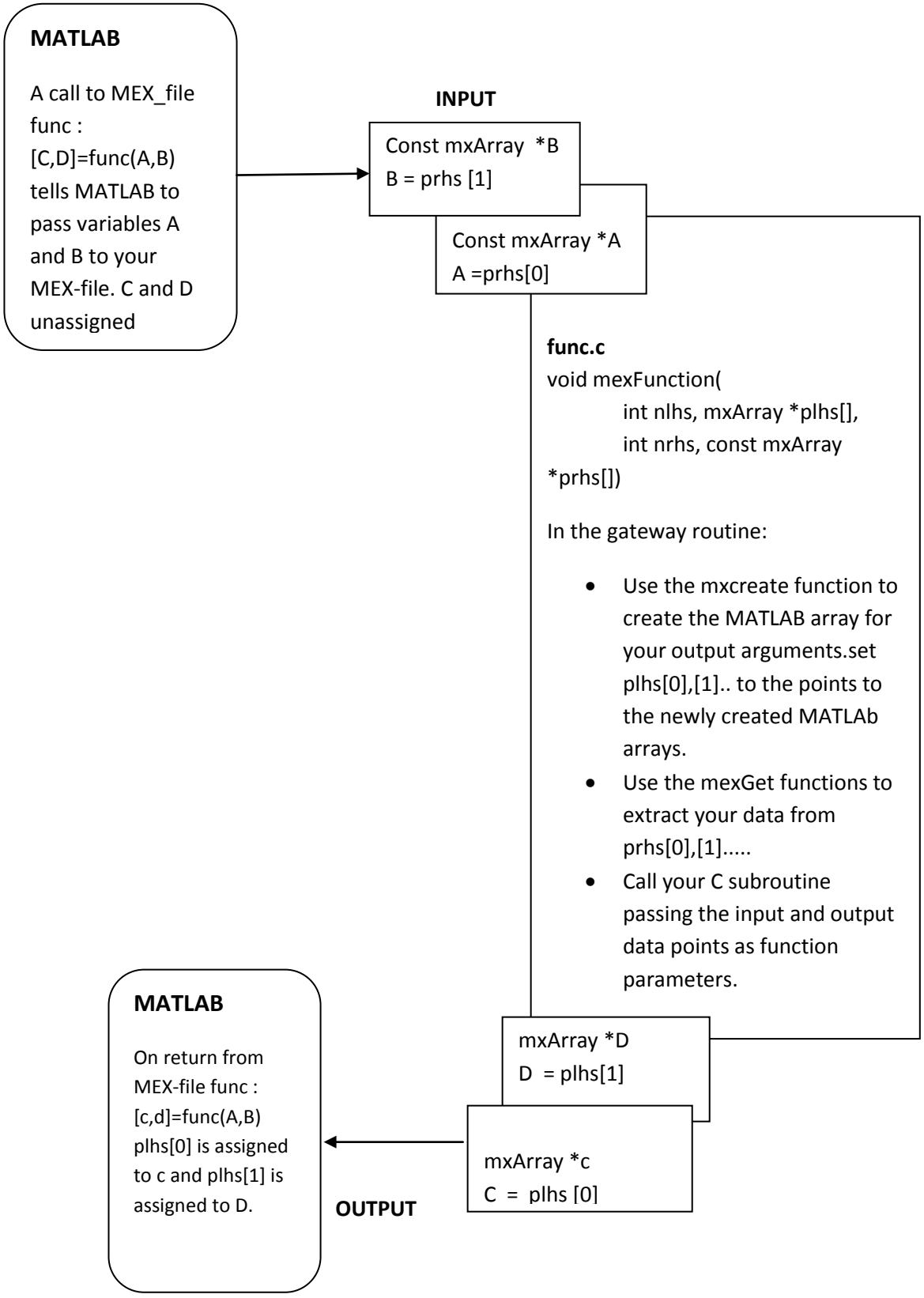

Figure 4.1: C MEX Internal Operation [12].

4.3 Working Procedure with Example

Create Mex Source File,

Create Gateway Routine,

Verify Input and Output Parameters,

Read Input Data,

Prepare Output Data,

Build the MEX-File.

These are the steps to be followed for creating and calling the MEX-File from Matlab [11].

4.3.1 Create Mex Source File

For example open Visual Studio 2008, create new Project and choose one *.c* templet name the templet as imageBoost used for enhancing the contrast of the image by using the functionality "trim_histtails_contrast_boost" the total functionality of the function "trim_histtails_contrast_boost" had been written in separate *c* file. This file is the computational routine and the name of the mex file is imageBoost.

4.3.2 Create Gateway Routine

At the beginning of the C file use the header

```
#include "mex.h"
```

Add the Gateway routime mexfunction and is of the form

```
void mexFunction(int nlhs, mxArray *plhs[], int nrhs,
const mxArray *prhs[])
{

idata = (unsigned char*)mxGetData(prhs[0]);//mxGetPr(prhs[0]);
ippmm = DEFAULT_PPI / (double)MM_PER_INCH;
id=8;
memcpy(y1,idata,mrows*ncols*sizeof(unsigned char));
/* ENHANCE IMAGE CONTRAST IF REQUIRED*/ argument
```

```
trim_histtails_contrast_boost(idata,mrows,ncols);

}
```

Parameters nlhs and nlhs contains number of left-hand side arguments and right-hand side arguments which invokes the MEX-File .

General form of Matlab functions can represented using the sintax

$$[a, b, c] = fun(d, e, f,)$$

Where a, b, c are left-hand arguments and d, e, f are right-hand arguments. Paramentes plhs and prhs are vectors that contain pointes to both lext and righ-hand side arguments. Thses are declared as type mxArray * .

For example consider a function

$x = fun(y, z)$; Which invoves MEX-Files from Matlab using the arguments

nlhs = 1

nrhs = 2

prhs is a 2-element C array where first element is a pointer to mcArray named y and second element named as z. plhs is 1-elemenr C array where the single element is null pointer and it is points to nouthing because the output x is not created untill subroutine executes.

4.3.3 Build the MEX-File

Build the MEX-File and change the path of the current directery of Matlab for accessing the executable file. Input parameters are passed from Matlab to executable file to perform total functionality. In this example a fingerprint image is passed from Matlab to executable file which performs image boosting operation and the output is given back to Matlab as shown in Fig. 4.2.

From MATLAB

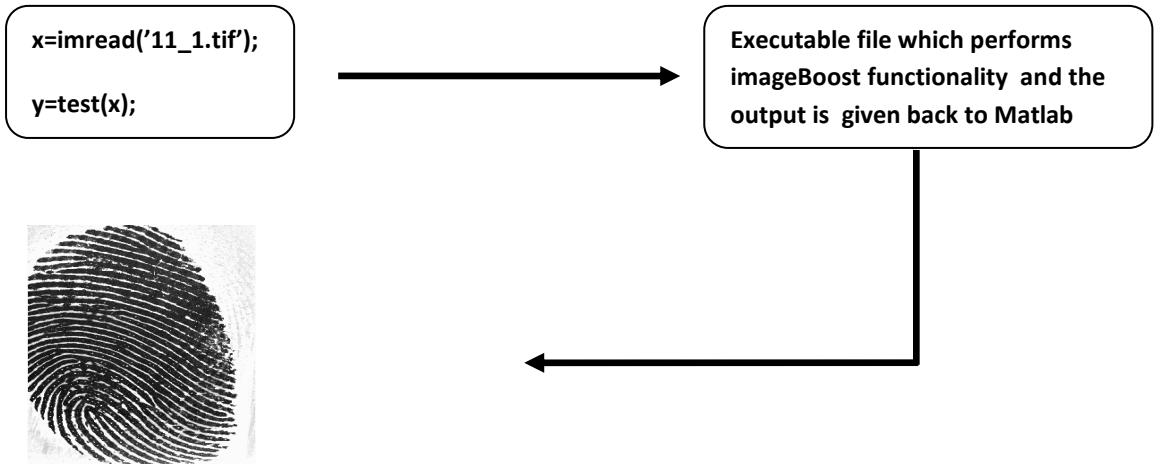

Figure 4.2: Flow of data between MATLAB and Visual Studio 2008 using MEX-Files.

Chapter 5

Receiver Operating Characteristics (ROC) Graphs

5.1 Introduction

Receiver operating characteristics (ROC) is a technique used for organizing classifiers and visualizing the performance. ROC graphs are frequently used in the areas of medical decision making, machine learning and data mining. In the machine learning community the usage of ROC graphs are increased. By considering the performance of the set of classifier a graph can be drawn which remains stable at derived conditions. The shape of the graph will also be change based on conditions of the classifier. So the annalist of that particular application will obtain an idea at which conditions which classifier is suitable. ROC graphs for example are applied in speech/music discriminations; it may be detection of speech and detection of music [8].

“In addition to begin a generally useful performance graphing method, they have properties that make them especially useful for domains with skewed class distribution and unequal classification error cost. These characteristics have become increasingly important as research continues into the areas of cost-sensitive learning and learning in the presence of unbalanced classes”[9].

5.2 Classification

Given a classifier and instance, there are four possible outcomes. If the instance is positive and the instant is classified as positive, it is considered as true positive; if the instance is classified as negative it is treated as false negative. If the instance is negative and the instance is classified as positive, it is considered as false positive; if the instance is classified as negative it is treated as true negative as shown in the Fig. 5.1 [9].

True Class

True Positive	False Positive	**Y**
False Negative	True Negative	**N**
P	**N**	

Hypothesized Class

Figure 5.1: Confusion matrix.

The true positive rate is the ratio of number of positives correctly classified (i.e. True Positive) by total number of positives in the classifier, also called as hit rate of the classifier is estimated as

$$\text{tp rate} \approx \frac{Positives\ correctly\ classified}{Total\ positives}. \tag{5.1}$$

The false positive rate of ratio of number of negative incorrectly classified (i.e. False Negative positive) by total number of negatives in the classifier, also called as false alarm rate of the classifier is estimated as

$$\text{fp rate} \approx \frac{Negative\ incorrectly\ classified}{Total\ Negatives}. \tag{5.2}$$

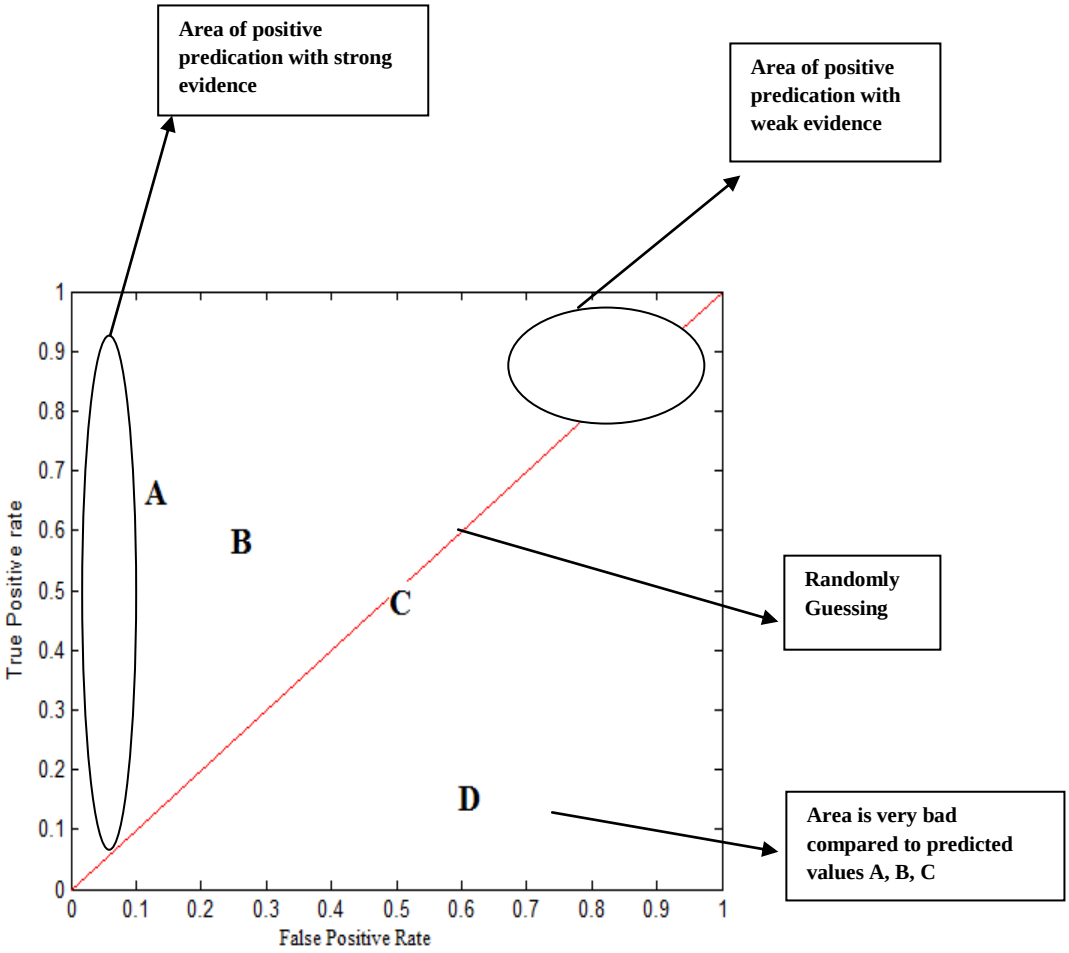

Figure 5.2: ROC curve with 4 predicted values from the classifier.

From the Fig. 5.2 the x −axes represents false positive rate and the y −axes represents true positive rate. The ROC graph shows four predicted values from A to D in the classifier, the point $(0,0)$ doesn't represent a positive classifier ,point $(0,1)$ represents perfect classification, the straight line represents random guessing, the area above the straight line is good for strong predication with strong evidence and the area below the line is totally in inverse (worse predication).In the figure from the predicted vales A, B, C, D. Here A and B clearly represents the good performance where A is far better than B and C lies on the diagonal line (random Guessing) and finally performance of D is too bad when compared to all the three (A, B, C).

5.3 Area under ROC Curve (AUC)

Performance of the classifier can be depicted using ROC curve. For comparing classifiers performance, a common method is to calculate the area under the ROC curve (AUC). AUC is the position of unit squire, its value varies between 0 and 1. Random guessing creates a value between (0,0) and (1,1), which has a area of 0.5.

Fig. 5.3 shows the area under ROC curves of A and B. Classifier A has greater area compared to classifier B, so the performance of the A is better compared to B performance. Performance of the classifier with high AUC is less in some cases compared to the classifier with low AUC. In Fig. 5.3 classifier A is generally better than B except at False Match rate > 0.25 where B has slightly high area.

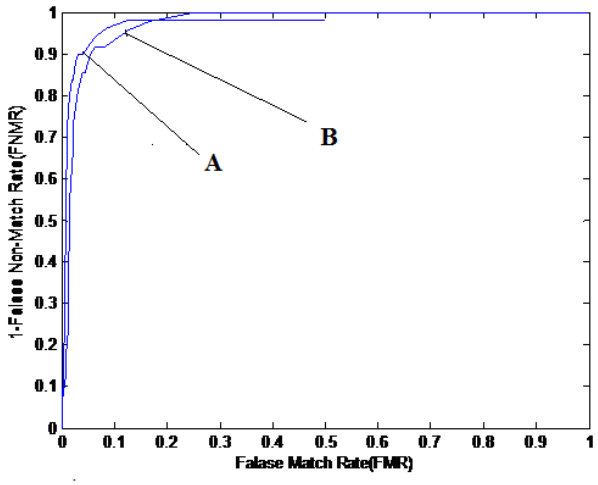

Figure 5.3: AUC of two classifiers A and B.

5.4 Evaluating accuracy of biometric system using ROC graphs

Evaluation of Biometric system accuracy is based on matching score distributions of identical and non-identical fingerprints. Suppose that biometric template is represented as T and the acquired input as I. Then null and alternate hypothesis are: $H0$: $I \neq T$, input does not come from same person as the template;

$H1: I = T$, input comes from same person as the template.

$D0$: person who is not claims to be;

$D1$: person who claims to be.

If the matching score $s(T, I)$ is greater than the threshold t then the score is categorized into $D1$, else it is categorized into $D1$. According to the communication theory main goal is to detect the message from noise. $H0$ is the hypothesis where the received signal is noise and $H1$ is the hypothesis where the received signal is message and noise. Such hypothesis testing contains two types of errors:

Type1: false match ($D1$ is decided when $H0$ is true);

Type2: false non-match ($D0$ is decided when $H1$ is true).

False Match Rate (FMR) is the probability of type1 error and False Non-Match Rate (FNMR) is the probability of type2 error. Fig. 5.4 graphically illustrates FMR and FNMR over genuine and imposter distribution.

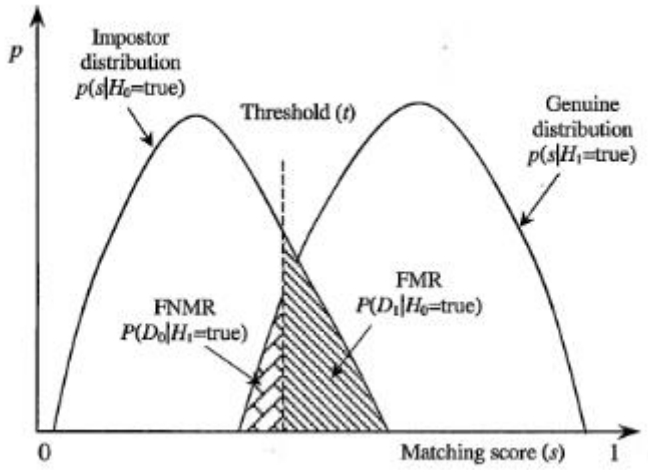

Figure 5.4: FNR and FNMR for a given threshold t.

FMR is area under imposter pairs for the threshold greater than or equal to t, FNMR is area under genuine pairs for the threshold less than or equal to t [1]. From the Fig.5.4 scores greater than or equal to threshold (t) is known as FMR (Imposter pairs) and whose matching score less than t is known as FNMR (Genuine pairs).

$$FNMR = \int_0^t p(s/H_1 = true)ds \quad (5.1)$$

$$FMR = \int_0^t p(s/H_0 = true)ds. \quad (5.2)$$

Both FMR and FNMR are functions of threshold (t). As the value of t decreases FMR (t) increases and the system becomes more tolerant to noise which may lead high probability to imposters to get in. The system becomes more secure when the value of t increases, then FNMR (t) increases. By using ROC graphs we can represent the system performance at all points of t. It helps the system designer to observe the system performance at all points so that the system can be used for particular applications at particular values of t[1].

FMR and FNMR are different for differ applications, for some applications highFMR is considered and for some applications lowFMR (highFNMR) is considered. For example in forensic applications such as criminal identification false non-match rate is concern because a genuine person (criminal) shouldn't be escaped. In very high secure applications low false match rate is considered because imposter may not be allowed. In between these two extremes there exists a condition where both false match rate and false non-match rate are considered. For example in ATM card verification high false match may leads to loss of several hundred dollars and high false non-match rate may irritate the customers. Fig. 5.5 illustrates the trade of between FMR and FNMR between different applications [1].

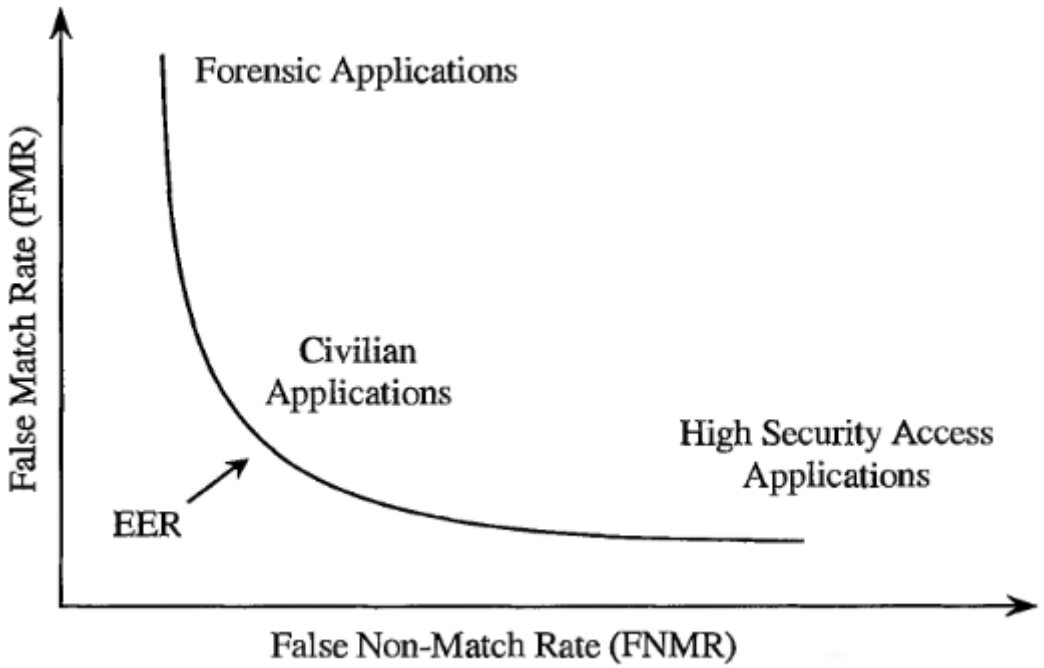

Figure 5.5: Typical operating of different applications displayed on a ROC curve.

From the Fig. 5.4, Fig. 5.6

- Genuine Match
  Match between two samples of the same fingerprint.
- Imposter Match
  Match between two different Fingerprints.
- False Accept Rate (FAR)
  Falsely accepting an imposter match.
- False Reject Rate (FRR)
  Falsely rejecting a genuine match.
- Equal-Error Rate: The point at which FMR and FNMR are identical i.e. $\mathrm{FMR}(t) = \mathrm{FNMR}(t)$.
- ZeroFMR is the point at which false matcher occurs.
- ZeroFNMR is the point at which no false matcher occurs.

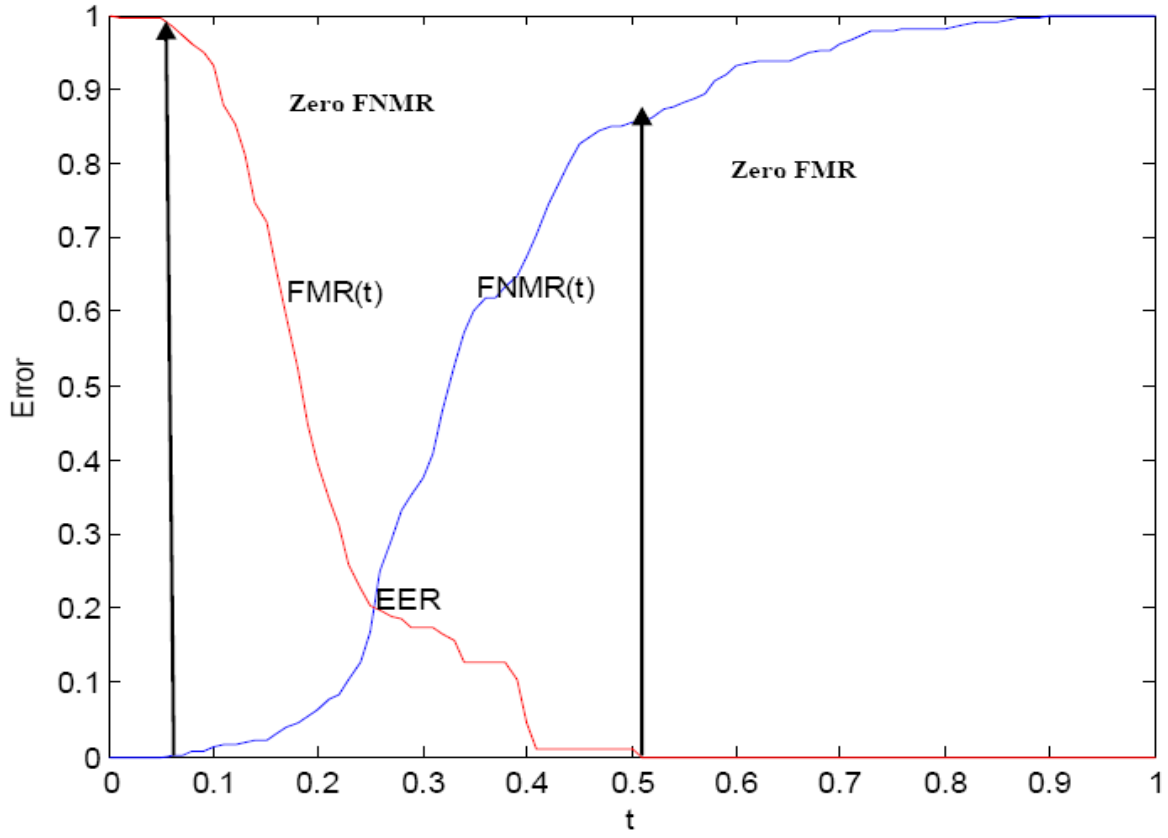

Figure 5.6: ROC curve between FMR and FNMR where EER, ZeroFMR and ZeroFNMR are highlighted.

5.5 Experimental Results

"FVC 2000 Database1_a" [17] was used to evaluate the NIST software in this thesis. This Database consists of 100 users fingers with 8 different samples from each finger. Among 100 different fingers top 60 users with 8 different samples from each finger are used in this work. This type of database is used to evaluate the fingerprint matching at different conditions. ROC graphs of FNMR is calculated from 60 different fingers with 8 different samples from each user of genuine attempts. A single image of the 8 samples I compared to rest of the 7 fingerprint for the same user. FMR is calculated for 60 different fingers with 8 different samples from each finger of imposter matching in which each fingerprint is matched with all imposter images.

For FNMR it will be around 3500 combinations,

For FMR it will be around 67319 combinations.

As explained in section 5.4 based on the vales of *t* the system becomes more tolerant to noise and more secure. So the system performance is reported at all operating points(threshold, *t*). Scores obtained from FNMR and FMR are plotted using ROC graphs so that the performance of the Biometric system can be identified. If we plot the scores obtained from different biometric systems with that curve a genuine system can be identified at different points of thresholds [10].

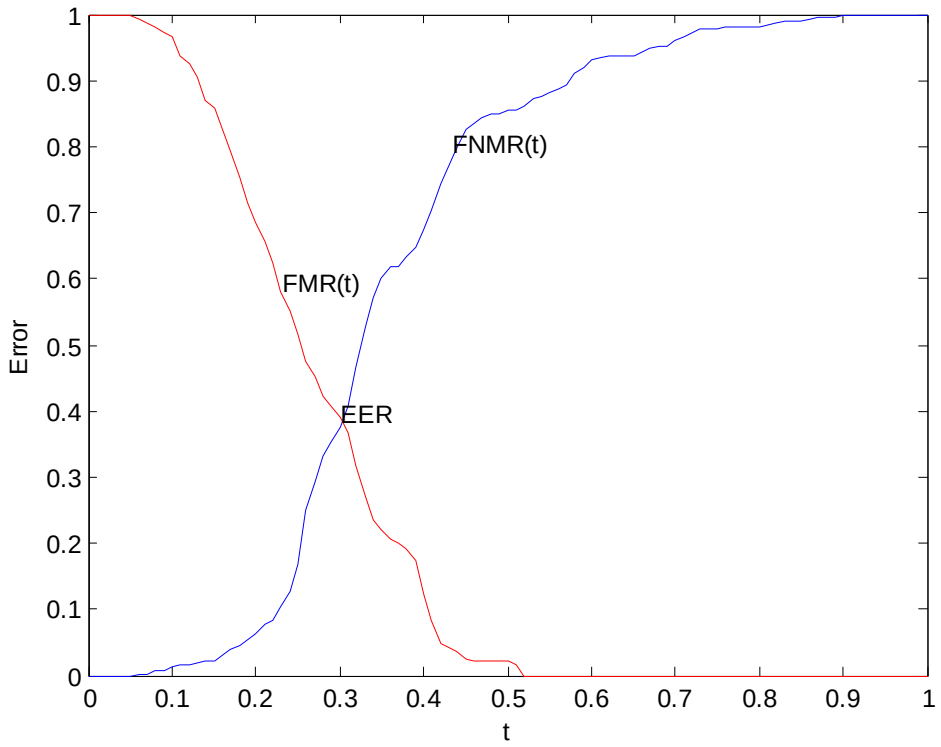

Figure 5.7: Plotting FMR (t) and FNMR (t) obtained from Genuine and imposter distributions (3500 genuine pairs and 67319 imposter pairs).

Results displayed below shows the ROC curve for the proposed algorithm for NIST software. Fig. 5.7 specifies FMR(t) and FNMR(t) obtained from Genuine and imposter distributions which resembles with the ROC-curve shown in Fig. 5.6. Fig. 5.8 evaluates the performance of the system i.e. area under ROC curve as explained in section5.3. For evaluating the performances of two systems same plot is made for the scores obtained for different technique using same DB and the system with more AUC is treated as best system.

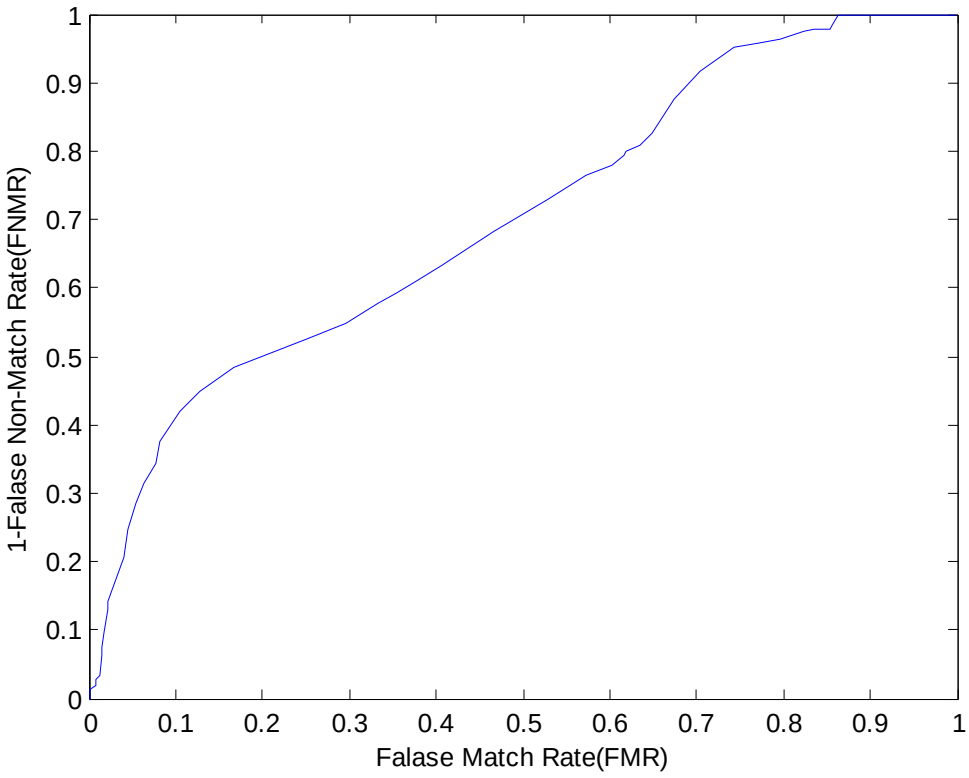

Figure 5.8: Plotting FMR(t) and 1-FNMR(t) obtained from Genuine and imposter distributions (3500 genuine pairs and 67319 imposter pairs).

Chapter 6

Conclusion

NBSI source code for fingerprint recognition which is entirely written in ANSI $\boldsymbol{C}$ programming language is implemented and evaluated by using the system developed in Matlab environment. This is performed by using $\boldsymbol{C}$ language MEX-files which enables to run original $\boldsymbol{C}$ code without reimplementing it as Matlab script. A function is developed with NBIS which helps to extract minutiae from grayscale fingerprint image and match two minutiae patterns to produce a match score. In this work 60 unique users with 8 fingerprints per user i.e., 480 fingerprints had been used for evaluating the system. Scores obtained from minutia matcher after comparing with genuine and imposter matching had been plotted using Receiver Operating Characteristic (ROC) graphs.

Finally the performance of the system is evaluated by analyzing plotted Receiver Operating characteristics (ROC) graphs. The results obtained by using this functionality can be used for comparing the results obtained with other technique for measuring the system performance (same DB is used in both cases) using ROC graphs.

Bibliosgraphy

[1] D. Maltoni, D. Maio, A.K. Jain and S. Prabhakar, Handbook of Fingerprint Recognition, Springer, 2003, ISBN 0-387-95431-7.

[2] The central source of information on biometrics-related activities of the Federal government, available at http://www.biometrics.gov/Documents/FingerprintRec.pdf.

[3] NIST Biometric Image Software, available at http://fingerprint.nist.gov/NBIS/nbis_non_export_control.pdf.

[4] I A. Jain, L. Hong and R. Bolle, "On-Line Fingerprint Verification", IEEE Trans. Pattern Analysis and Machine Intelligence, Vol. 19, No.4, pp. 302-3 14, Apr. 1997.

[5] Ahmad, F.; Mohamad, D.; "A Review on Fingerprint Classification Techniques", International Conference on computer Technology and Development, ICCTD '09, Vol.2, pp. 411-415, 2009.

[6] NIST special databases and software from the image group, available at http://www.itl.nist.gov/iad/894.03/databases/defs/dbases.html.

[7] Signal Detection theory handout, available at, http://www-psych.stanford.edu/~lera/psych115s/notes/signal/.

[8] Alnadabi, M.; Johnstone, S.; , "Speech/music discrimination by detection: Assessment of time series events using ROC graphs," Systems, Signals and Devices, 2009. SSD '09. 6th International Multi-Conference on , vol., no., pp.1-5, 23-26 March 2009

[9] Tom Fawcett,"ROC Graphs: Notes and Practical Considerations for References", available at http://home.comcast.net/~tom.fawcett/public_html/papers/ROC101.pdf.

[10] K.; Morita, A.; Aoki, T.; Higuchi, T.; Nakajima, H.; Kobayashi, K.; , "A fingerprint recognition algorithm using phase-based image matching for low-quality fingerprints," Image Processing, 2005. ICIP 2005. IEEE International Conference on , vol.2, no., pp. II- 33-6, 11-14 Sept. 2005.

[11] MATLAB Documentation for using MEX-Files to call C/C++ and Fortran Programs , available at http://www.mathworks.se/access/helpdesk/help/techdoc/matlab_external/f29502.html

[12] "Hand book for "Calling C and Fortran Programs from MATLAB" available at http://www.karenkopecky.net/Teaching/Cclass/MatlabCallsC.pdf.

[13] Asker M. Bazen, Gerben T.B. Verwaaijen, Sabih H. Gerez,Leo P.J. Veelenturf and Berend Jan van der Zwaag ," A Correlation-Based Fingerprint Verification System".

[14] Lavanya, B.N.; Raja, K.B.; Venugopal, K.R.; Patnaik, L.M.; , "Minutiae Extraction in Fingerprint Using Gabor Filter Enhancement," Advances in Computing, Control, & Telecommunication Technologies, 2009. ACT '09. International Conference on , vol., no., pp.54-56, 28-29 Dec. 2009

[15] User's Guide to NIST Biometric Image Software (NBIS) available at, http://www.nis.gov/cgi-bin//get_pdf.cgi?pub_id=51097

[16] User's Guide to Export Controlled Distribution of NIST Biometric Image Software (NBIS-EC) available at, http://fingerprint.nist.gov/NBIS/nbis_export_control.pdf.

[17] Maio, D.; Maltoni, D.; Cappelli, R.; Wayman, J.L.; Jain, A.K.; , "FVC2000: fingerprint verification competition," Pattern Analysis and Machine Intelligence, IEEE Transactions on , vol.24, no.3, pp.402-412, Mar 2002.

[18] Muhammed Umer Munir, Dr. Muhammed Younus Javed "Fingerprint Matching Using Gabor Filters".

[19] Anil K. Jain, Arun Ross and Salil Prabhakar "An Introduction to Biometric Recognition," Appeared in IEEE Transactions on Circuits and Systems for Video Technology, Special Issue on Image- and Video-Based Biometrics, Vol. 14, No. 1, January 2004.

[20] Dijana Petrovska-Delacrétaz, Gérard Chollet, Bernadette Dorizzi ; "Guide to Biometric Reference Systems and Performance Evaluation", Springer-Verlag London Limited 2009, ISBN 978-1-84800-291-3.